SUPPORTING INFORMATION

Natural Rubber - SiO_2 Nanohybrids: Interface Structure and Dynamics

Md. Abdul Sattar [a,b] * , A. Sreekumaran Nair [b] , P. J. Xavier [b] and Archita Patnaik [a]*

[a] Colloid and Interface Chemistry Laboratory, Department of Chemistry, Indian Institute of Technology Madras, Chennai-600036, India.

[b] *MRF Limited, R & D Centre, MRF Road, Tiruvottiyur, Chennai-600019, India.*

CONTENTS

1. ADDITIONAL EXPERIMENTAL DATA:

An optimum Mg^{2+} ion concentration of 100 mM enabled hetero-aggregation resulting in the nanocomposite formation. Nanocomposites prepared under low electrolyte concentration (< 100 mM) of Mg^{2+} ions remained turbid even after 24 h without complete hetero-aggregation.

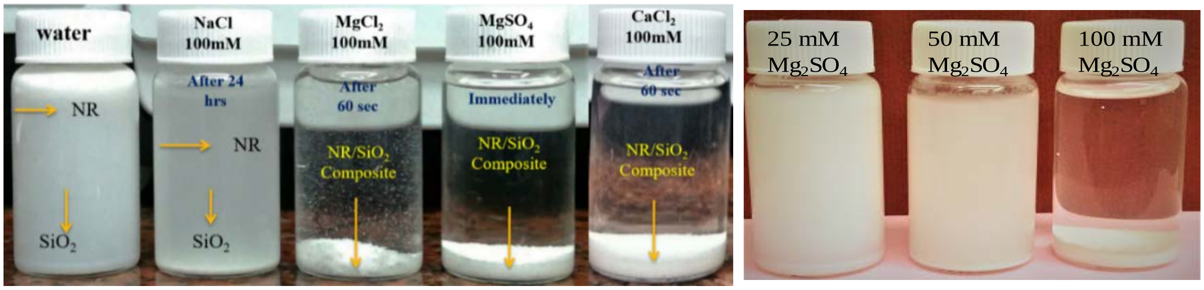

Figure S1: Depiction of nanoscopic aggregation in NR/SiO_2 nanocomposites in presence of different metal ions at 100 mM ionic strengths and at different Mg^{2+} electrolyte concentrations.

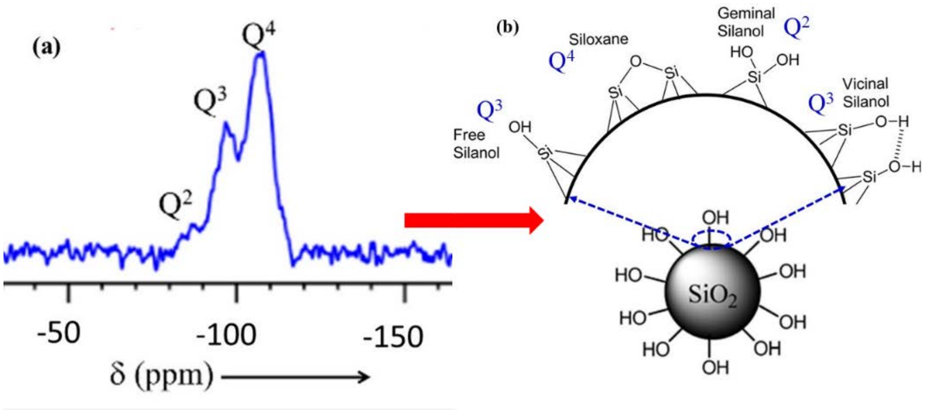

Figure S2: (a) Solid state CP/MAS ^{29}Si NMR of the synthesized SiO_2 NP, (b) scheme depicting possible types of silanol groups on SiO_2 surface.

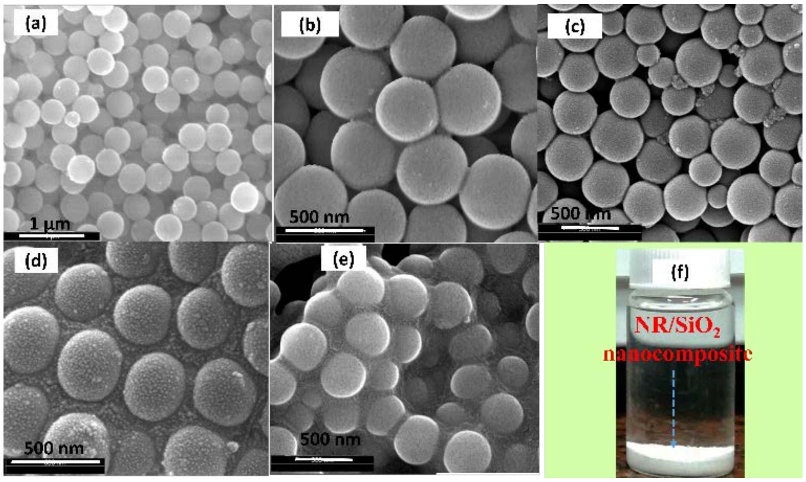

Figure S3 (I): HRSEM images of a) Pristine SiO_2 NP, (b-e) NR-SiO_2 nanocomposites as a function of percentage silica volume fraction; b) NR-52; c) NR-36; d) NR-30 and e) NR-16 and f) vial showing NR-SiO_2 hetero-aggregate composite formed by the addition of divalent Mg^{2+} cation.

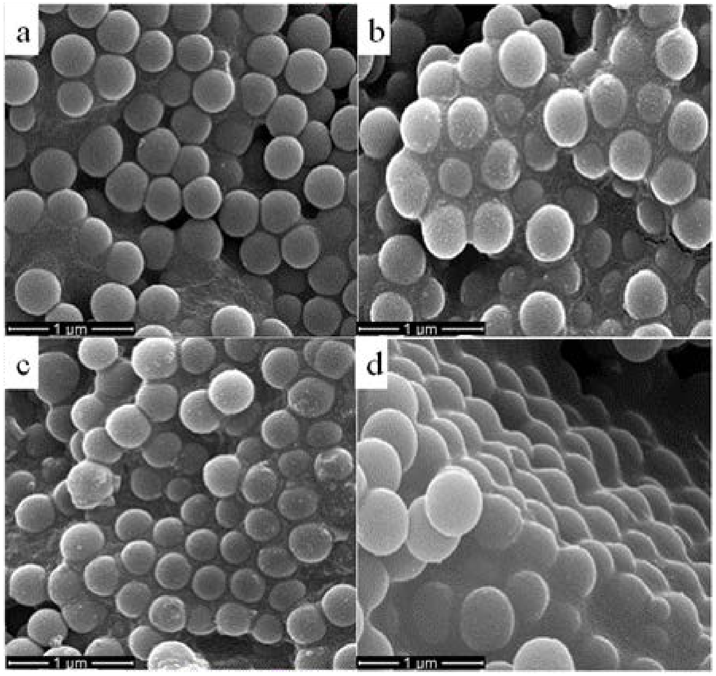

Figure S3(II): HRSEM images of NR-SiO_2 nanocomposites as a function of percentage silica volume fraction; a) NR-52; b) NR-36; c) NR-30 and e) NR-16

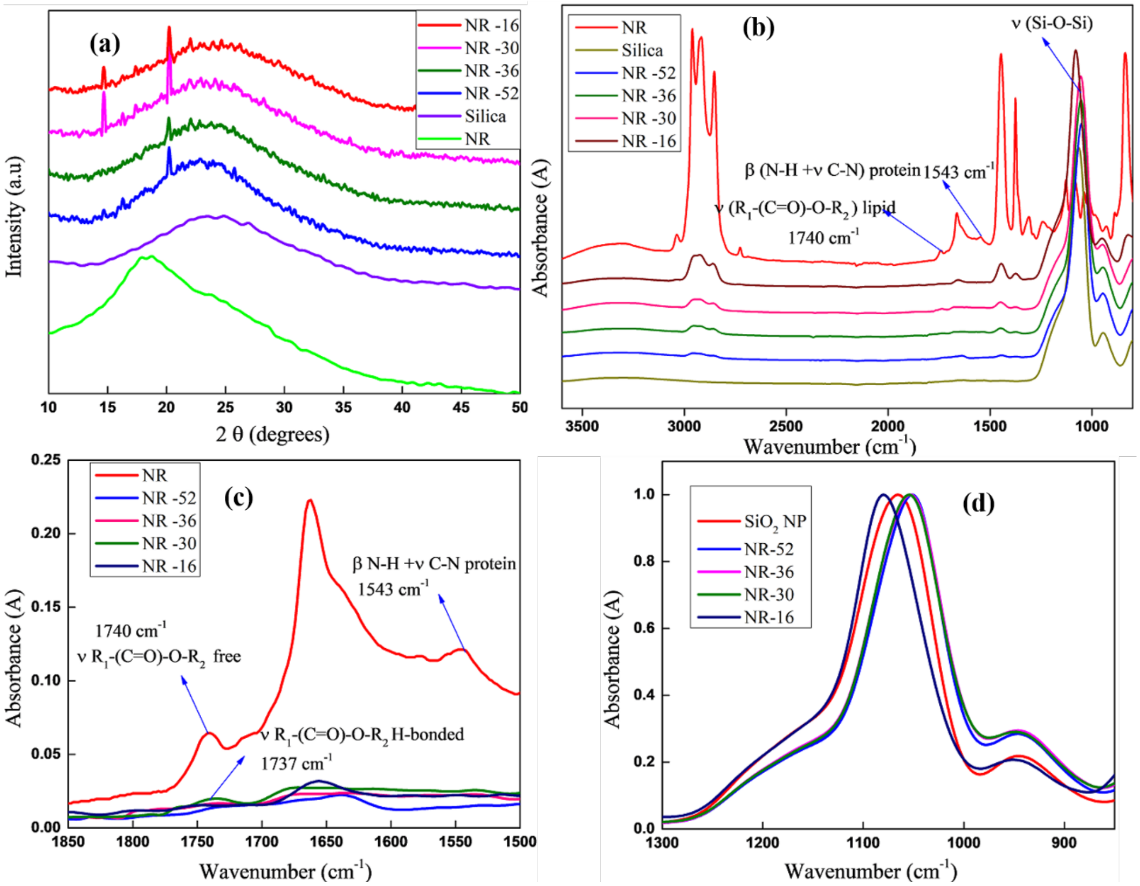

Figure S4: a) WAXD profiles of NR, Silica and NR-SiO_2 nanocomposites with various silica volume fractions, b) FT-IR Spectra of NR, SiO_2, and NR-SiO_2 nanocomposites, c) FT-IR Spectra of neat NR and NR-SiO_2 composites depicting the H-bonding in the ester and amide regions of NR d) FT-IR Spectra of pristine SiO_2 and NR-SiO_2 composites depicting the changes in asymmetric Si-O-Si stretching frequencies in silica region.

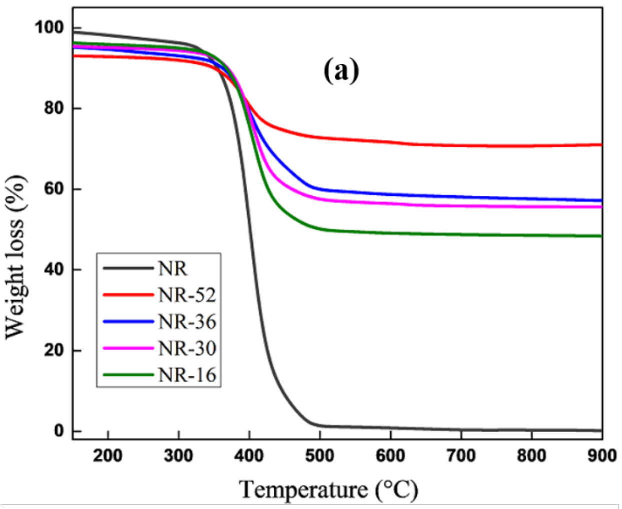

Figure S5: TGA thermograms of bulk and adsorbed NR on SiO_2 NPs as a function silica volume fraction (a) normal and (b) derivative mode.

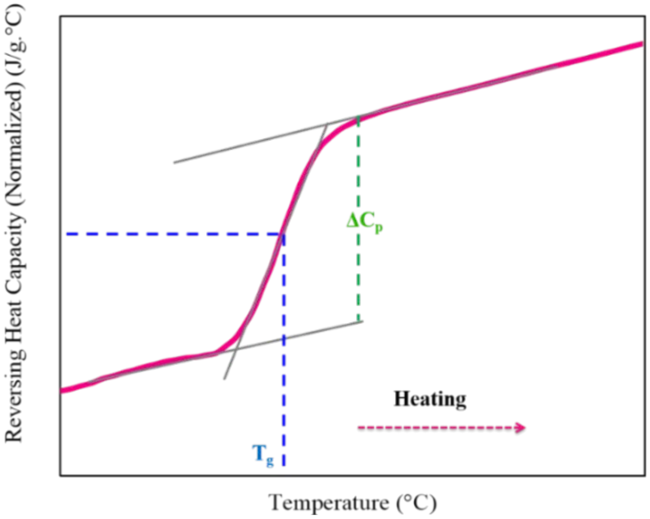

Figure S6: Estimation of specific heat capacity of the composite at the glass transistion temperature T_g from TMDSC experiments.

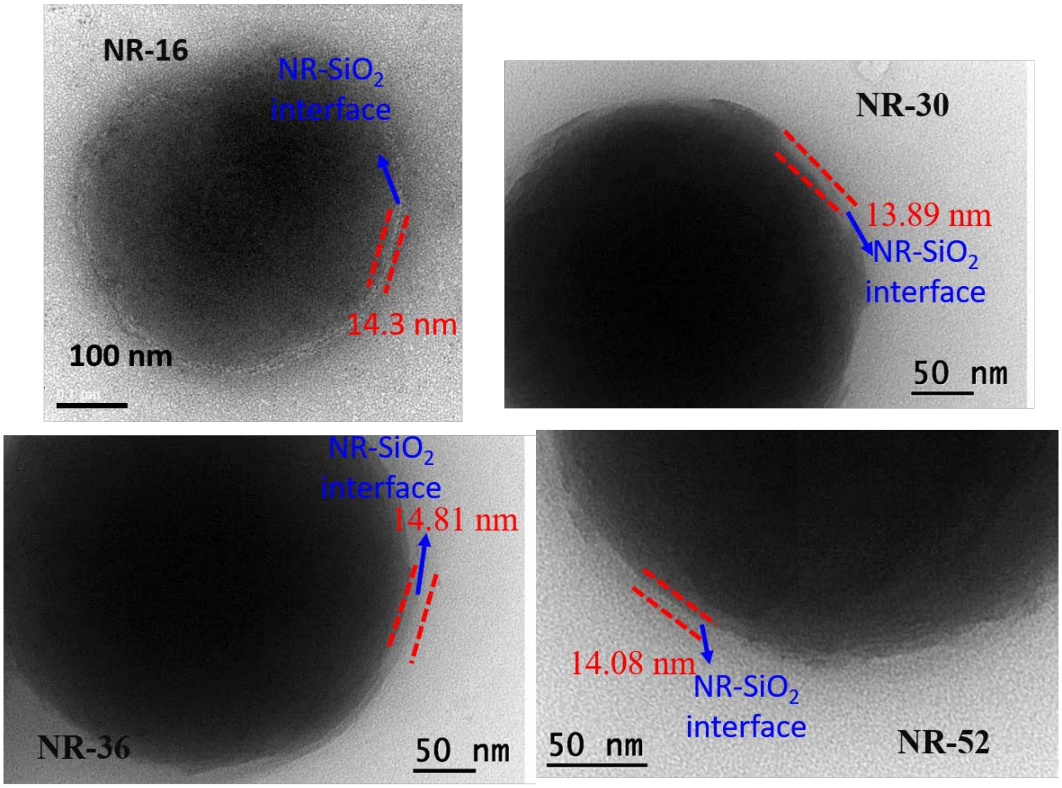

Figure S7: TEM images depicting the core-shell structure of NR/SiO_2 nanocomposite with estimated interface thickness.

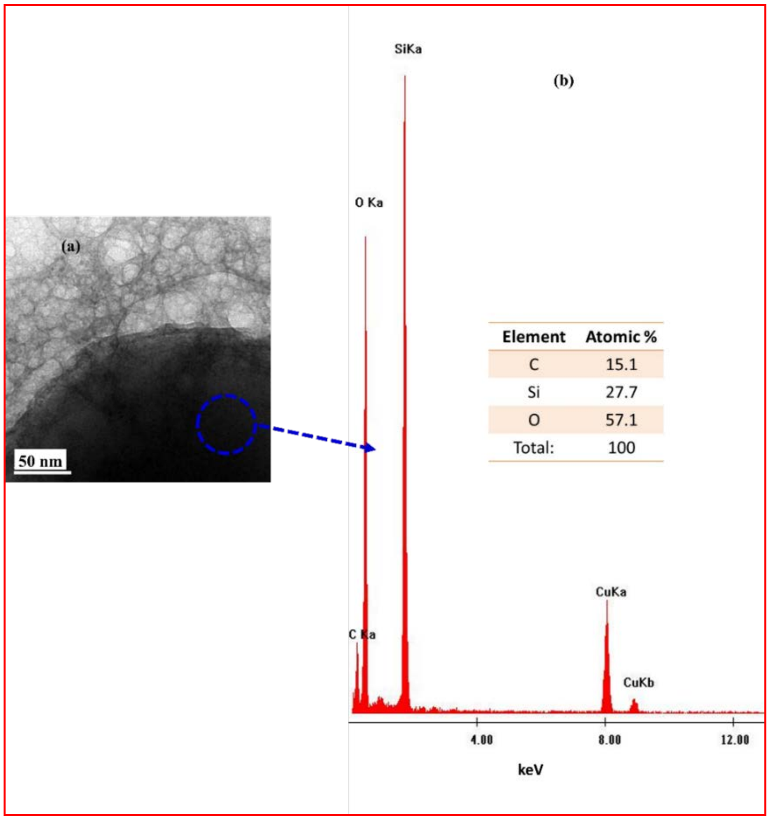

Element	Atomic %
C	15.1
Si	27.7
O	57.1
Total:	100

Figure S8: TEM image (a) followed by the EDAX spectrum (b) of the SiO_2 core of the nanocomposite

Silica Surface Texture and Interfacial Layer Thickness in the Nanocomposite: The effects of silica surface texture on the interfacial layer thickness were studied by preparing nanocomposite with commercially available micron sized silica (cf. Figure S6(a-c). The normalized specific reversing heat capacity curves of these nanocomposite at T_g shown in Figures S6 (c-d) indicate both types of SiO_2 particles showing depression in T_g compared to the pure NR. Moreover, the change in the specific heat capacity jump is smaller for the nanocomposite obtained from the micron sized SiO_2 than the Stöber SiO_2 NP. An extended T_g step in the specific heat capacity of nanocomposites with commercial micron size silica indicates the presence of a larger interfacial layer with higher thermal stability. This difference is attributed to the surface textural features of SiO_2, as listed in Table S1. Although surface to volume ratio is high in case of nano SiO_2 with identical total number of silanol groups as that in commercial micron size silica, larger pore volume and diameter of the latter enable physical and mechanical entrapment of polymer chains, resulting in a dead polymer layer with occluded NR exhibiting slower segmental dynamics than the isolated polymer.

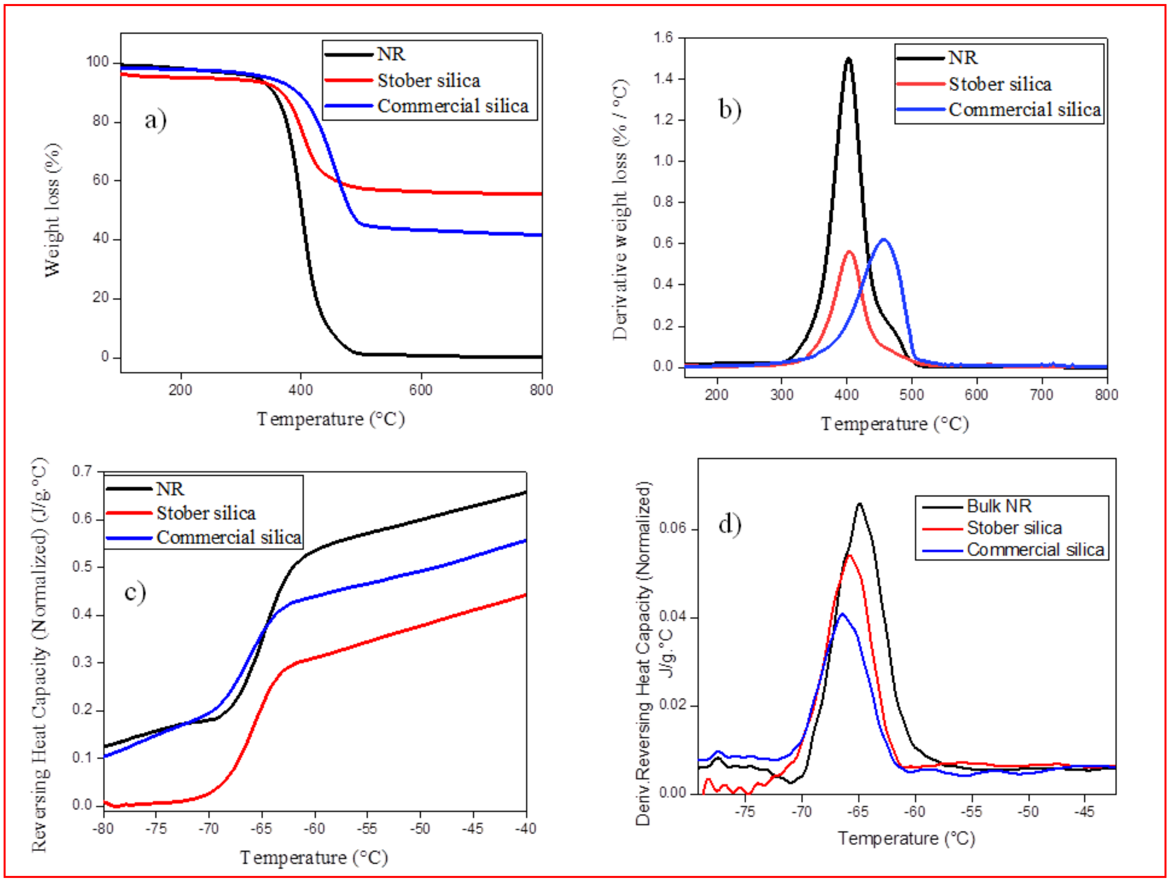

Figure S9 a), b) TGA and DTA of bulk and adsorbed NR on commercial silica and Stöber silica under similar silica and polymer concentrations. c) Normalized specific reversing heat capacity and d) the derivative curves of the respective NR and the composites during glass transition.

Table S1. Surface area and pore size analysis of synthesized Silica NPs and commercial silica.

	Specific surface area (m^2/g)	Pore volume (cc/g)	Pore diameter Å	# OH /nm^2
Stöber silica	319	0.32	30	8.4
Commercial silica	193	0.42	78.5	8.3

2. ADDITIONAL COMPUTATIONAL DATA

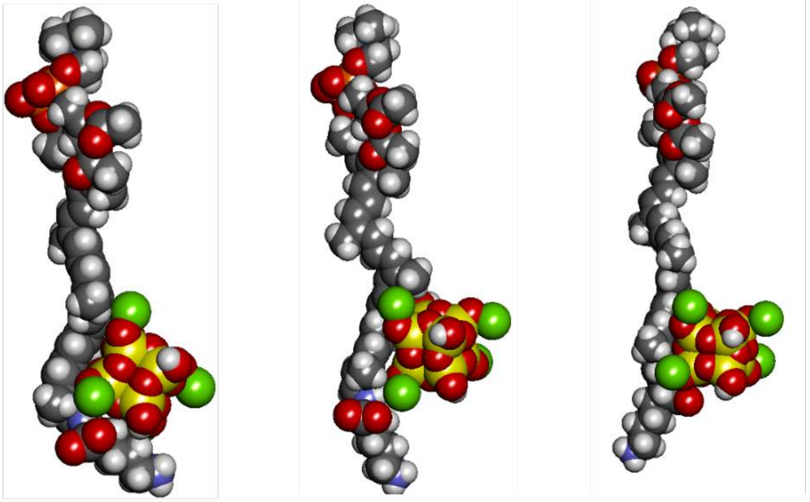

(a) Mg.....O distance = 1Å
E = 149.9 kcal/mol

(b) Mg.....O distance = 2Å
E = 145.2 kcal/mol

(c) Mg.....O distance = 3Å
E = 142.0 kcal/mol

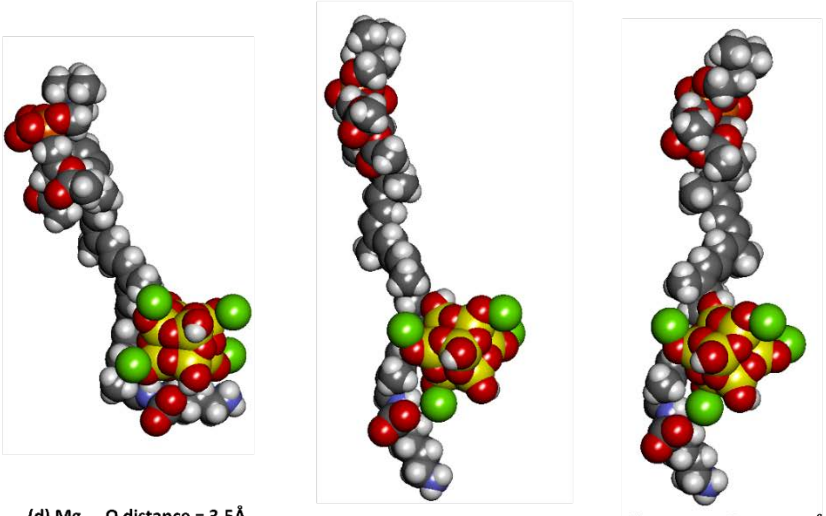

(d) Mg.....O distance = 3.5Å
E = 132.3 kcal/mol

(e) Mg.....O distance = 4Å
E =140.8 kcal/mol

(f) Mg.....O distance= 5Å
E =141.9 kcal/mol

Figure S10: MM+ geometry optimized structures of model nanocomposites simulated using NR and silica cluster, whose chemical structures are shown in Figure 2. The snapshots are shown by varying the distance between the lysine carboxylic oxygen atom (126) of NR and Mg (34) atom of silica cluster. A minimum energy configuration was obtained at a distance of 3.5 Å.

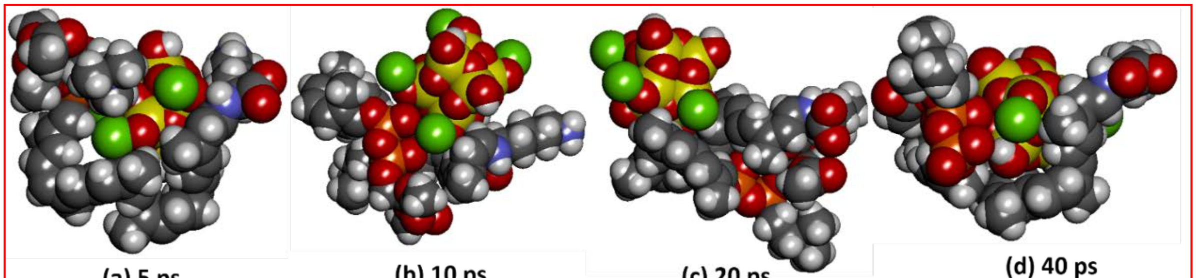

(a) 5 ps
E = 498.8 kcal/mol

(b) 10 ps
E = 492 kcal/mol

(c) 20 ps
E = 485.6 kcal/mol

(d) 40 ps
E = 450.4 kcal/mol

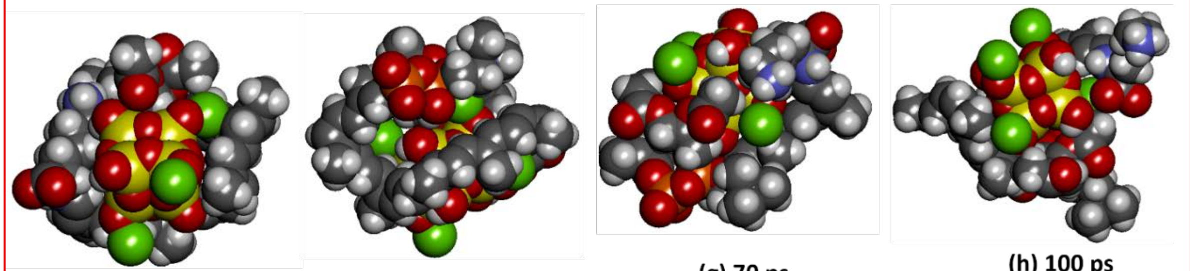

(e) 45 ps
E = 426.2 kcal/mol

(f) 50 ps
E = 439.8 kcal/mol

(g) 70 ps
E = 480.7 kcal/mol

(h) 100 ps
E = 482.2 kcal/mol

Figure S11: Snapshots of the simulated NR-SiO_2 composite structures after 5-100 ps. The core-shell structure stabilization is seen after 45 ps.

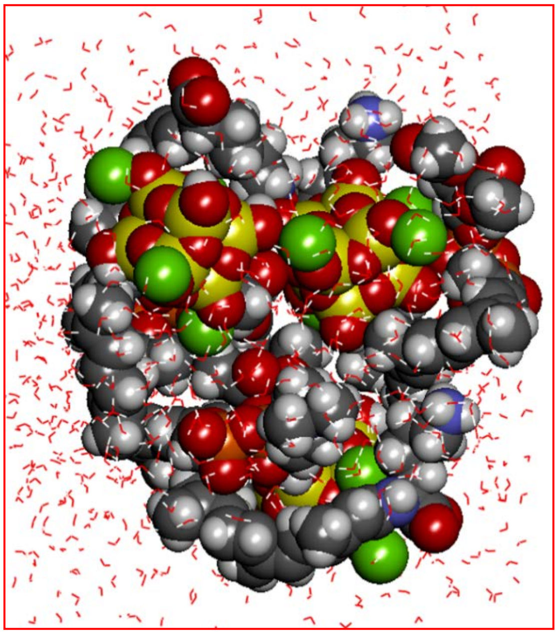

Figure S12: Snapshot of the simulated structure of a 3-unit NR/SiO_2 nanocomposite model in a periodic boundary box after 30 ps with energy E = 3182.3 kcal/mol. The number of water molecules filling the 35 × 35 × 35 Å^3 boundary box = 1416.